Vegetation control on nutrient availability and supply in high-elevation tropical Andean ecosystems

Armando Molina[1,2], Veerle Vanacker[3], Oliver Chadwick[4], Santiago Zhiminaicela[5], Marife Corre[1], and Edzo Veldkamp[1]

[1]Soil Science of Tropical and Subtropical Ecosystems, Faculty of Forest Sciences and Forest Ecology, University of Göttingen, Göttingen, Germany.

[2]Facultad de Ciencias Agropecuarias, Universidad de Cuenca, Campus Yanuncay, Cuenca, Ecuador.

[3]Earth and Life Institute, Centre for Earth and Climate Research, University of Louvain, 3 Place Louis Pasteur, B-1348
10   Louvain-la-Neuve, Belgium.

[4]Department of Geography, University of California, Santa Barbara, Santa Barbara, CA 93106-4060, USA.

[5]Subgerencia de Operaciones, Agua Potable y Saneamiento, Empresa Pública Municipal de Telecomunicaciones, Agua Potable, Alcantarillado y Saneamiento de Cuenca (ETAPA EP), Cuenca, Ecuador.

Correspondence to: A. Molina (Armando.molinav@ucuenca.edu.ec). Facultad de Ciencias Agropecuarias, Universidad de
15   Cuenca, Campus Yanuncay, Cuenca, Ecuador. V.Vanacker (veerle.vanacker@uclouvain.be). Earth and Life Institute, University of Louvain, Louvain-la-Neuve, Belgium.

Abstract.

Plants absorb nutrients and water through their roots, and modulate soil biogeochemical cycles. The mechanisms of water and nutrient uptake by plants depend on climatic and edaphic conditions, as well as the plant root system. Soil solution is the medium in which abiotic and biotic processes exchange nutrients, and nutrient concentrations vary with the abundance of reactive minerals and fluid residence times. High-altitude ecosystems of the tropical Andes are particularly interesting to study the association between vegetation patterns, soil hydrology and soil nutrient availability. The páramo landscape forms a vegetation mosaic of bunch-grasses, cushion-forming plants and forests. In the nutrient-depleted nonallophanic Andosols, the plant rooting depth varies with drainage and soil moisture conditions. Vegetation composition is a relevant indicator of rock-derived nutrient availability in soil solutions. The soil solute chemistry revealed patterns in plant available nutrients that were not mimicking the distribution of total rock-derived nutrients nor the exchangeable nutrient pool, but clearly resulted from strong biocycling of cations and removal of nutrients from the soil by plant uptake or deep leaching. Our findings have important implications for future management of Andean páramo ecosystems where vegetation type distributions are dynamically changing as a result of warming temperatures and anthropogenic disturbances. Such alterations may not only lead to changes in soil hydrology and solute geochemistry but also to complex changes in weathering rates and solute export downstream with effects on nutrient availability in Andean rivers and high-mountain lakes.

1 Introduction

35 Plants absorb nutrients and water through their roots, and modulate soil biogeochemical cycles (Kelly et al., 1998; Jackson et al., 2002; Amundson et al., 2021). The availability of soil nutrients regulates terrestrial primary productivity (Chadwick et al., 1999; Vitousek, 2004; White et al., 2012a; Uhlig et al., 2020). In young ecosystems, plant-essential mineral nutrients such as calcium (Ca), potassium (K), magnesium (Mg), phosphorus (P), and silica (Si) are derived from mineral weathering of rock and soil, that releases rock-derived nutrients into the biological environment (Chadwick et al., 1999; Hedin et al., 2003; Dixon

40 et al., 2016). As the store of primary minerals is consumed during soil development, the nutrient supplying capacity decreases. When the nutrient supply from lithogenic sources declines, biocycling of essential nutrients by plants becomes more important (Landeweert et al., 2001; Vitousek et al., 2003). Thus nutrient acquisition and water uptake by plant roots drive the circulation of water and dissolved nutrients within the critical zone (Uhlig et al., 2017; Rempe and Dietrich, 2018), while litterfall, root decay, and decomposition release nutrients and make them bioavailable again (Hobbie, 1992; Amundson et al., 2007).

45

Soil solution is the medium in which abiotic and biotic processes exchange nutrients (Niemenen et al., 2013; Olshansky et al., 2019). Nutrient concentrations in shallow soil water are recharged by biological processes and vary seasonally with vegetative growth cycles (White et al., 2012a) that depend on temperature and rainfall. Biologically essential nutrient concentrations are often highest in the upper soil horizons, a result of mineralization and deposition processes (Jobbágy and Jackson, 2001, 2004).

50 In contrast, nutrient concentrations in deeper soil water increase with depth, a result of mineral weathering and exchange processes, due to the abundance of reactive minerals and longer fluid residence times (Brantley and White, 2009; White et al., 2012a).

The mechanisms of water and nutrient uptake by plants depend on climatic and edaphic conditions (Porder et al., 2009), as

55 well as the plant root system, especially the plant rooting depth (Schenk and Jackson, 2002). Plants typically take up soil water using shallow roots, although deep roots can play a key role in acquiring water and nutrients from deeper soil horizons and redistribute them to shallower horizons, particularly during drought (Brantley et al., 2017; Hasenmueller et al., 2017; Dawson et al., 2020). In well-drained aerated upland, soils and plant rooting typically follow infiltration depth, whereas in waterlogged anaerobic soils, often shallow roots develop (Fan et al., 2017). Plant rooting depth can, in turn, influence soil hydrology through

60 transpiration losses and water uptake (Cramer et al., 2008), chemical weathering (Canadell et al., 1996; Rempe and Dietrich, 2018), and regulate long-term carbon storage and soil nutrient distributions (Jackson et al., 2000).

Despite the importance of biological and geochemical processes in regulating nutrient availability in terrestrial ecosystems, few studies have addressed the role of vegetation communities and soil hydrology in soil nutrient availability. High Andean

65 tropical ecosystems provide a good opportunity to study the association between vegetation patterns, soil hydrology and soil nutrient availability: the climate, parent material, and soil age can be held constant at the landscape scale, while the vegetation

and soil hydrology can vary greatly from the hilltops to the valley bottoms. High-altitude grassland ecosystems of the tropical Andes are particularly interesting because persistently cool temperatures of 2 to 10 °C, mean annual precipitation above 500 mm, low transpiration rates and frequent fog which give rise to low soil microbial decomposition rates (Ramsay, 1992;

70 Tonneijck et al., 2010). Moderate to highly weathered uniform soils (Podwojewski and Poulenard, 2000; Molina et al., 2019) are prevalent, and they are rich in organic matter content (Minaya et al., 2016). Carbon sequestration is particularly remarkable leading to important soil carbon sinks (Hribljan et al., 2016; Comas et al., 2017). High Andean rivers have a particular stream load as their dissolved load exceeds the suspended solid load during normal hydrological years (Tenorio et al., 2018). The elevated dissolved organic carbon concentrations cause extra acidy in water with consequences on the aquatic ecology of rivers

75 and high-mountain lakes (Mosquera et al., 2022).

In this study, we evaluated the association between vegetation, soil hydrology and mineral nutrient availability at the landscape scale. It is part of a larger group of studies on soil-water-vegetation interactions in tropical volcanic ecosystems that all used the same sampling scheme for maximum inter-site comparability (Molina et al., 2019; Páez-Bimos et al., 2022). The site in

80 the southern Ecuadorian Andes is underlain by andesitic parent material, and soils experience only limited input of Holocene distal tephra (Rodbell et al., 2002). External soil nutrient input from e.g. dust and ocean-salt aerosols can be assumed to be minimal. We measured nutrients over the course of one hydrological year in soil pore water solutions, under different combinations of vegetation, soil moisture and drainage conditions. Specifically, our research addressed the following questions: (1) How does vegetation regulate soil moisture, drainage and soil development? (2) How are soil moisture conditions

85 related to the availability of rock-derived nutrients (Ca, K, Mg, Na, P and Si) in the soil solution? and (3) How does vegetation influence the relative availability of nutrients. The study is based on a new dataset containing data on soil solution chemistry and soil water potential collected over a full hydrological year, and was complemented with data on soil bulk chemistry and soil hydraulics.

2 Site description

90 Our study was carried out at the Cuevas catchment (4.2 km²), located in a grassland (or so-called páramo) ecosystem on the western Cordillera in southern Ecuador, about 30 km northwest of the city of Cuenca (3°01'50" S, 79°17'59" W, Molina et al., 2019). Altitudes range from 3608 to 3960 m above sea level, with gently sloping (< 12%) valley bottoms and steeper slopes (12-25%) on the hillsides. The glaciated landscape was shaped during the Pleistocene giving rise to frequently observed glacial features such as moraines, U-shaped valleys and glacial lakes (Jantz and Behling, 2012). The site is part of an area that is

95 protected by the public drinking water company (ETAPA EP). This high-altitude páramo ecosystem has an udic moisture regime and an isomesic temperature regime (Poulenard et al., 2003; Buytaert et al., 2005). The annual rainfall (1998-2013 period) averaged 911 mm at the Soldados meteorological station (3500 m a.s.l., ETAPA EP), and exhibits a bimodal regime (Mora and Willems, 2012). As rainfall is associated with cloudiness, there is also a continuous moisture input from clouds and

fog. The air temperature is seasonally constant with a mean annual air temperature of about 8°C (ETAPA EP). Although the

100 mean temperature shows little seasonal variation, there are strong diurnal variations with a maximum temperature of 18 °C

during the day and a minimum temperature of 1°C during the night. Because of the low temperature and year-round air

humidity, the evapotranspiration is low and estimated at 45 to 60% of the total annual rainfall (Carrillo-Rojas et al., 2019;

Lazo et al., 2019).

105
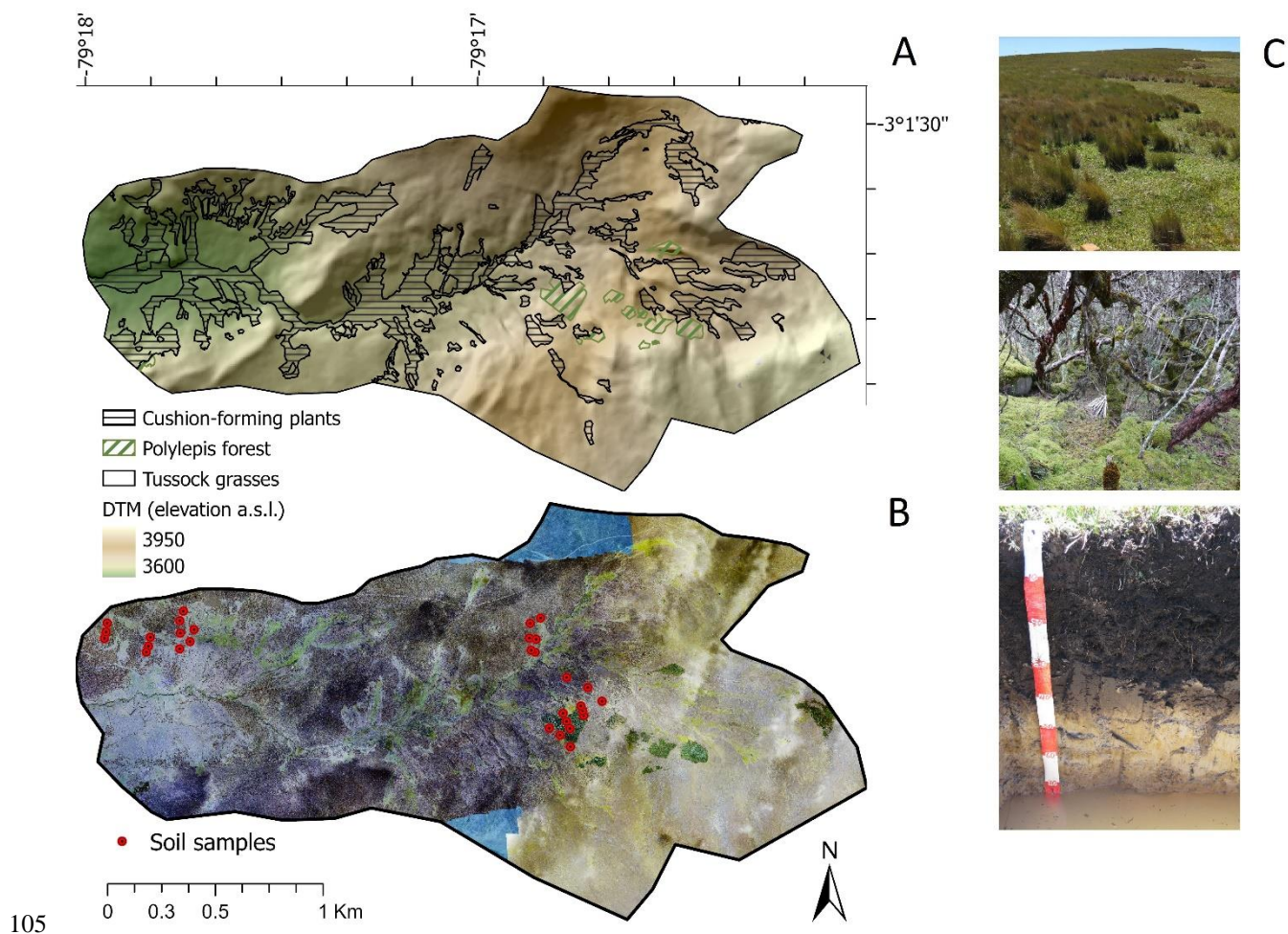
Figure 1: Overview of the three main vegetation assemblages in the high-altitude páramo ecosystem, with abundance of cushion-forming plants in topographic hollows and valley bottoms, tussock grasses along the hillsides and forest in poorly accessible areas. (A) Representation of the topography with indication of the three vegetation types. (B) Colour composite of the aerial photographs taken with an indication of the location of the soil profiles. (C) Examples of the vegetation types, and one selected soil profile showing

110 **the importance of organic matter accumulation. The topographic and land use information was derived from aerial photographs taken by an uncrewed aerial vehicle using UAV-PPK-SfM techniques following Clapuyt et al. (2016) and Zhang et al. (2019).**

Summits and hillslopes have well-drained soils covered by bunch or tussock grasses, whereas toeslopes and valley bottoms are characterized by permanently waterlogged areas covered by cushion-forming plants. Forest patches are present on poorly

115   accessible and steeper terrain in the upper part of the catchment. Plant communities in the tussock-grass páramo consist mainly of bunch-grasses of the genera *Stipa* and *Calamagrostis* (Poaceae) (Jantz and Behling, 2012) and include Poaceae (*Paspalum*, *Cortaderia*), Hypericaceae (*Hypericum*), and Valerianaceae (*Valeriana*). Páramo wetlands are covered by cushion-forming plants, which comprise species of Plantaginaceae (*Plantago rígida*) and Cyperaceae (*Uncinia*) (Jantz and Behling, 2012; Coblentz and Keating, 2008). Woodlands contain small trees of 3 to 5 m height with the dominant species *Polylepis reticulate*

120   (Fig. 1). Extensive grazing (by cattle and horses) had an impact on the landscape, but slowed down after 2010 when the land was declared a protected area. Traditional burning of grasslands is still practised in the wider region to remove old grass and allow nutritious, vigorous, new shoots to grow (White, 2013).

The nonallophanic Andosols developed on andesitic parent material from the Mio-Pliocene (Beate et al., 2001; Podwojewski

125   and Poulenard, 2000; Buytaert et al., 2006). Soil formation started after the parent material was exposed following the retreat of glaciers during the late Pleistocene (Hansen et al., 2003). The young, postglacial soils experienced intense weathering with strong depletion of the Ca, Na, and K base cations throughout the soil depth (Molina et al., 2019). The presence of allophane is very limited, and soils are dominated by metal-humus complexes. The organic horizons have soil bulk densities as low as 0.28 g cm^{-3} and an organic carbon content up to 21%. Beyond the hillslope-scale topographic control on soil development,

130   chemical and physical properties of soils differ by the soil weathering intensity and the type of vegetation. Soil depth (defined as depth to C horizon) varies across the vegetation communities, with average soil depths of 65 cm for tussock grasses, 61 cm for forest, and 42 cm for cushion plants. Relative to the parent material, forest soils are strongly depleted in base cations (with total mass losses of 1440 kg.m^{-2}) followed by soils under tussock grasses (1210 kg.m^{-2}) and under cushion plants (1170 kg.m^{-2}). Soil acidity is enhanced by weathering, with a soil pH$_{H_2O}$ of 4.8 under forests, 5.0 under tussock grasses and 5.6 under

135   cushion plants. Detailed information on the chemical weathering and soil development was reported earlier (Molina et al., 2019).

3. Materials and methods

3.1. Soil sampling strategy

Within the 4.2 km² study area, 33 sampling locations were selected: 9 under native polylepis forest, 9 under cushion-forming

140   plants and 15 under the dominant vegetation cover, tussock grasses. Automatic weather station (Cancan Refugio, 3692 m a.s.l., ETAPA EP) records rainfall, air temperature and relative humidity. Soil pits were excavated to a depth of more than 15 cm below the soil weathering front, reaching depths of 57 to 120 cm. We sampled and described the soil profiles based on genetic horizons following the procedures of the World Reference Base for Soil Resources (Food and Agriculture

145 Organization, 2006). Information on plant rooting depth was derived from field measurements during soil profile descriptions, and a distinction was made between the effective and the maximum rooting depth. The effective rooting depth corresponds to the zone where most of the roots grow in the upper horizons, and the maximum rooting depth to the deepest rooting depth observed in the C horizons. Soil and rock chemical analyses are described in Molina et al. (2019), and we re-used here the data on the exchangeable base cations and mass transfer coefficients (Table 1 and 3 in Molina et al., 2019) to assess the retention of rock-derived nutrients in the soil system. As the soil profiles have variable thicknesses, the bulk soil data were recalculated

150 for multiple depth intervals of 20 cm each to facilitate inter-site comparison following the approach of Jobbágy and Jackson (2001).

3.2. Determination of soil hydro-physical properties

We derived the volumetric soil moisture content, bulk density and water retention for a selection of 12 profiles: 3 under

155 polylepis forest, 3 under cushion-forming plants, and 6 under tussock grasses. The A and C horizons of these profiles were sampled by taking undisturbed samples of 100 cm³ (in triplicate) in stainless steel rings and disturbed samples (700 g) in zip lock bags. Soil water retention curves were then determined from the experimental data on soil water retention for different matric potentials at the soil hydro-physical laboratory of PROMAS at the Universidad de Cuenca. Soil water retention at lower matric potentials (-100, -300, and -1500 kPa) was measured on saturated disturbed samples. Samples were mixed with water

160 to a saturated soil paste which was then preserved in a closed container for 1 week. The soil paste was then placed in PVC rings on a pressure membrane in a container in which different pressures were applied, and samples are left for 7 days to equilibrate before measurement (Klute, 1986). At high matric potentials (0, -3, -6, -10, -24, and -46 kPa), the water retention was determined on undisturbed samples by the multi-step apparatus (van Dam et al., 1994). To estimate the gravimetric water content (g g^{-1}) for a given matric potential (kPa), the samples were weighted. At the end of the experiment, the samples were

165 oven-dried at 80°C during 48 hours, and weighted again to obtain the soil bulk density (g cm^{-3}). This information was then used to convert the gravimetric water content (g g^{-1}) into volumetric water content (cm³ cm^{-3}). The soil water retention curves (12 sites × 2 horizons) were obtained by fitting a bimodal Van Genuchten model (Van Genuchten, 1980) through the measured soil water retention data following the approach described in Páez-Bimos et al. (2023).

170 Saturated hydraulic conductivity (K_s) of soils was measured in-situ on the A and C horizons of the 12 selected profiles using the inverse auger hole or so-called Porchet method (van Hoorn, 1979). We selected this method because of its extensive use in soils of páramo ecosystems (e.g. Buytaert et al., 2005; Marín et al., 2018, Páez-Bimos et al., 2022). The measurements were performed in fresh bore holes with 3 replicates per site. For further analyses, the average of the three measurements was taken.

3.3. Soil and rain water sampling

175 We sampled soil pore water using suction cup lysimeters (P80 ceramic, maximum pore size 1 μm; CeramTec AG, Marktredwitz, Germany). The 33 lysimeters were installed sub-horizontally at 50 cm depth, about 1 m upslope of the soil pits ~~at 50 cm depth~~. At this depth, they collect soil solutions from the upper soil horizons of the strongly weathered nonallophanic Andosols that are rich in organic matter as a result of biological activity including bioturbation and root growth (Molina et al., 2019). Rain water was sampled at the Cancan Refugio meteorological station where samples were collected with a plastic

180 funnel connected to a 1 L bottle that was wrapped in aluminum paper and stored in a closed plastic bucket underground. The top of the funnel was covered with a 1 mm mesh, and a 20 μm nylon mesh was placed between the funnel and the hose. Lysimeters, tubes, and collection bottles were acid-washed and rinsed with deionized water before installation. The collection bottles (from dark glass) were closed with rubber stoppers, placed in plastic buckets with lids and buried in the ground approximately 2 m downslope of the lysimeters. After an initial 2-month equilibration period, soil water was sampled every 2

185 to four weeks from October 2012 to September 2013. Soil water was collected by applying a vacuum of 40 kPa to the collection bottles (Schwendenmann and Veldkamp, 2005; Kurniawan et al., 2018). During sample collection, the collected water was transferred to a clean high-density polyethylene bottle of 100 mL.

We measured the soil moisture potential in-situ using tensiometers (P80 ceramic, maximum pore size 1 μm; CeramTec AG,

190 Marktredwitz, Germany). They were installed at the same depth as the lysimeters (50 cm) and at short distance (1 to 2 m). Soil water potential in the field was measured at the same time as soil water sampling, over the period October 2012 to September 2013. The data were converted into volumetric soil moisture values using measured soil water retention curves.

3.4. Soil water chemistry

Water samples were taken to the soil laboratory of the Faculty of agricultural sciences at the University of Cuenca (Ecuador)

195 and frozen immediately. The frozen samples were transported by air to the University of Göttingen (Germany) where the chemical analyses were conducted. Analyses of total dissolved N (TDN), NH_4^+, NO_3^- and Cl^- were conducted using continuous-flow injection colorimetry (AA3; SEAL Analytical, Norderstedt, Germany); Dissolved organic C (DOC) was analyzed using a total organic carbon analyzer (TOC-Vwp; Shimadzu Europe, Duisburg, Germany). Analysis of base cations and total dissolved Al, Fe, Mn S, P and Si was done using an inductively coupled plasma-atomic emission spectrometer (iCAP 6300;

200 Thermo Fischer Scientific, Dreieich, Germany). For details and detection limits we refer to Kurniawan et al. (2018). We reported all solute concentrations in $\mu mol_c\ L^{-1}$ (molar concentration multiplied by the equivalent charge of the solute). A partial cation-anion charge balance of the major solutes (i.e., those with concentrations > 2 $\mu mol_c\ L^{-1}$) was performed, considering all pore water samples of a given vegetation type following the methods described in Kurniawan et al. (2018). The contribution of bicarbonates (HCO_3^-) and organic acids ($RCOO^-$) were estimated by subtracting the total anion charge from the total cation

205 charge, whereby the charge contributions of the total Al were assumed to be 3^+. Solute concentrations that exhibited very low

levels (i.e., total Fe, Mn, and P), and thus had minimal charge contribution were excluded from the calculations (following the method used by Hedin et al., 2003).

Given the lack of Cl-bearing minerals in the parent material, the pore water Cl concentrations were used to estimate
210   evapotranspiration rates and soil water fluxes. We used the approach of White et al. (2009) and Buss et al. (2017) to estimate soil hydrological fluxes from the chloride concentrations in rain and soil water. Assuming 1D vertical flow, the fluid flux density is calculated as the net difference between annual precipitation and evapotranspiration fluxes, and equal to the product of precipitation and the ratio of volume-weighted Cl concentration in precipitation to that in soil pore waters (Buss et al., 2017). The average infiltration rate was then calculated by dividing the fluid flux density by the product of the average porosity and
215   saturation, and the average fluid residence time by taking the ratio of the profile thickness and the infiltration rate. To evaluate the role of vegetation uptake on plant nutrient concentrations in the soil solution, we analyzed nutrient/Cl ratios. Chloride is not an essential nutrient and not actively assimilated by the vegetation (Boxman et al., 2008) and changes in the soil water Cl concentrations are thus mainly caused by difference in soil water balance if we assume that the Cl input through weathering and deposition does not vary between sites. An increase in nutrient/Cl ratios indicates an enrichment of the nutrient relative to
220   Cl, and a decrease a removal of the nutrient relative to Cl.

3.5. Statistical Analysis

We used linear mixed-effects (LME) models (Crawley, 2009) to assess whether solute chemistry and soil hydrology are different in soils covered by cushion-forming plants, tussock grasses and polylepis forest. The model used the vegetation type as the fixed effect, and the spatial replication (experimental sites) and monitoring time (biweekly or monthly measurements)
225   as random effects. In total, 360 samples from 31 experimental sites were used for the statistical analysis, as we excluded the data from two forested sites (FR1 Middle, FR3 Upper) where exceptionally high solute concentrations were measured, larger than two standard deviations above the average. Differences between vegetation types (fixed effects) were assessed based on analysis of variance at p ≤ 0.05. Correlation between explanatory variables were tested with Spearman's rank correlation statistics, and we reported the strength and type of association by the Spearman's rho and p-values. The R software version
230   3.1.2 (R Development Core Team, 2014) was used to perform all the statistical analysis.

4. RESULTS

4.1. Variations in soil and vegetation rooting depth in páramo ecosystems

The young volcanic soils were generally thin and the depth to the C horizon ranged from 27 to 100 cm. Soils under cushion-forming plants were thinner (i.e., 42 ± 6 cm) than under forests (61 ± 17 cm) and tussock grasses (65 ± 19 cm, Table 1 in
235   Molina et al., 2019). The effective rooting depth of the vegetation was lower under cushion-forming plants than under forests or tussock grasses with depths of 33 ± 4 cm under cushion plants, and about 10 cm more in forests (44 ± 6 cm), and tussock

grasses (41 ± 8 cm, Fig. 2). The maximum rooting depth followed the same pattern with 51 ± 8 cm under cushions, 82 ± 16 cm under forest, and 75 ± 17 cm under tussock grasses (Table S1). The root systems of trees and tussock grasses allow the plants to acquire water and nutrients at significantly greater depths than cushion-forming plants. Some of the deepest roots extended to more than 1 m in well-drained soils developed under forest or tussock grasses. Effective and maximum root depths were positively associated to the soil depth, illustrating the strong link between soil development, plant growth and root development (Spearman's rho = 0.78 and 0.75 resp., p-value < 0.01, n = 31).
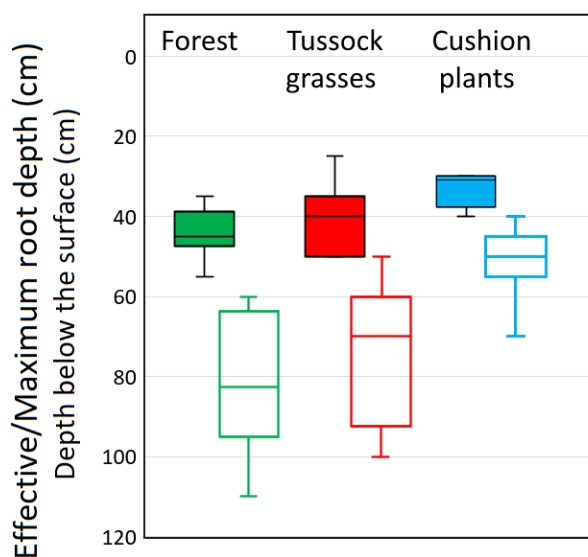
Figure 2: Root development in forests (n=9, green), under tussock grasses (n=15, red) and cushion-forming plants (n=9, blue). The effective rooting depth corresponds to the zone where most of the roots grow in the upper horizons, and the maximum rooting depth to the deepest rooting depth observed in the C horizons.

4.2. Nutrient distribution in the soil profile

All soils experienced intense chemical weathering with significant elemental depletion throughout the soil profile (Fig. 3). Total weight losses by chemical weathering for the 30 profiles ranged between 793 and 1610 kg.m^{-2}, with a mean value of 1240 ± 210 kg.m^{-2} (Table 3 in Molina et al., 2019). Depletion profiles did not show a clear trend in base cation loss with depth and had a rather uniform depletion of Ca, Na, K, and Mg throughout all horizons. The chemical mass losses were significantly different between vegetation types: soils covered by cushion-forming plants had the lowest chemical mass losses. Being significantly less depleted in Ca, Na, and K, their remaining stock of rock-derived nutrients was higher than in soils under forests and tussock grasses. The lithogenic elements that were biotically cycled by plants - Ca, K and Mg - had the highest concentrations of mean exchangeable cations in the upper 20 cm of the profiles, and then decreased with depth up to 60 cm (Fig. 3). This pattern was observed under all vegetation types and we inferred that they were being biotically pumped to the surface horizons. The lowest concentrations of exchangeable and total Ca and K were measured between 60 and 80 cm depth

which corresponds to the average maximum rooting depth. The exchangeable Ca and Mg concentrations varied between
260   vegetation types (Table 1). Soils under cushion plants had 82% higher exchangeable Ca and ~72 to 62 % higher exchangeable
Mg concentrations than under forests or tussock grasses (Table 2). In contrast to the Ca, K and Mg soil cations, the Na cation
concentration increased with soil depth under cushion plants although the absolute depth-variations were small. Similar to the
other biotically cycled elements, the exchangeable Na concentrations were significantly higher under cushion-forming plants.
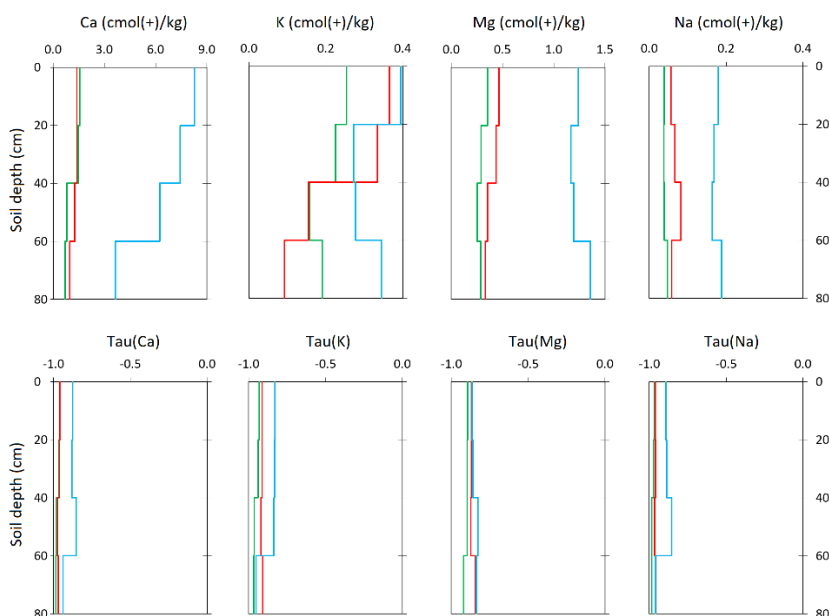
265

**Figure 3: Depth-variation of the mean exchangeable Ca, K, Mg, and Na concentrations, and their mean elemental mass transfer
coefficients in soils under forests (n=7, green line), tussock grasses (n=15, red line) and cushion-forming plants (n=9, blue line).**

Table 1. Summary of the linear mixed effect model, with indication of significance level of the fixed effects (vegetation type).

Nutrient/Element in soil solution	Cushion plants vs tussock grasses	Cushion plants vs forest	Tussock grasses vs forest
Calcium (Ca)	Y (< 0.001)	Y (< 0.001)	N (0.991)
Potassium (K)	N (0.827)	Y (< 0.050)	Y (< 0.010)
Magnesium (Mg)	Y (< 0.001)	Y (< 0.010)	N (0.845)
Sodium (Na)	Y (< 0.001)	Y (< 0.001)	N (0.906)
Total silica (Si)	Y (< 0.001)	Y (< 0.001)	N (0.740)
Total phosphorus (P)	N (0.801)	N (0.596)	N (0.774)
Total aluminum (Al)	Y (< 0.010)	Y (< 0.001)	Y (< 0.010)
Total Iron (Fe)	Y (< 0.010)	Y (< 0.001)	Y (< 0.010)
pH	Y (< 0.001)	Y (< 0.001)	Y (< 0.001)

270

Table 2: Mean annual concentration (± 1 SD) of the major elements in the soil solution under forest, tussock grasses and cushion-forming plants.

	Ca	K	Mg	Na	Si	P	Cl	S	Al	Fe	pH
	μM (mean ± 1 SD)										
Forest	28±18	38±28	14±7	69±50	18±22	0.2±0.1	20±4	11±4	13±8	1±0	5.7±0.6
Tussock grasses	19±7	11±8	9±3	58±29	39±38	0.3±0.3	15±10	4±1	2±1	1±2	6.5±0.2
Cushion plants	82±36	17±10	24±10	181±81	291±135	0.2±0.1	20±9	4±2	1±1	3±3	7.1±0.2

275

4.3. Soil hydrological properties

4.3.1. Spatiotemporal variation in soil moisture content

The annual rainfall measured at Cancan Refugio was 546 mm, about 40 % less than the mean annual rainfall in this region (ETAPA EP). The monitoring period (October 2012 to September 2013) coincided with a severe drought and 2012 and 2013

280 were amongst the driest years on record. Most of the rain (71%) fell during the wet season (i.e., between November 2012 and May 2013, Fig. 4) although April was unusually dry. The soil moisture pattern followed the overall rainfall seasonality with highest volumetric water contents in the wet season between November and June, and the lowest values between July and October. Despite the unusually low precipitation amount registered over the monitoring period, the volumetric soil water content remained high in all 33 soil profiles (i.e. above 0.40 $cm^3.cm^{-3}$, Table S1) and rather constant over the wet season and

285 it declined only gradually during the dry months. The temporal variation in soil moisture content was similar for all vegetation types, with below-average SWC values over the dry months. Clear differences were observed in the absolute soil moisture content between vegetation types: over the monitoring period, the volumetric soil water content under cushion-forming plants was, on average, 7% higher than under tussock grasses and 16% higher than in forests (Fig. 4). Forests experienced more water stress than cushion plants and tussock grasses.
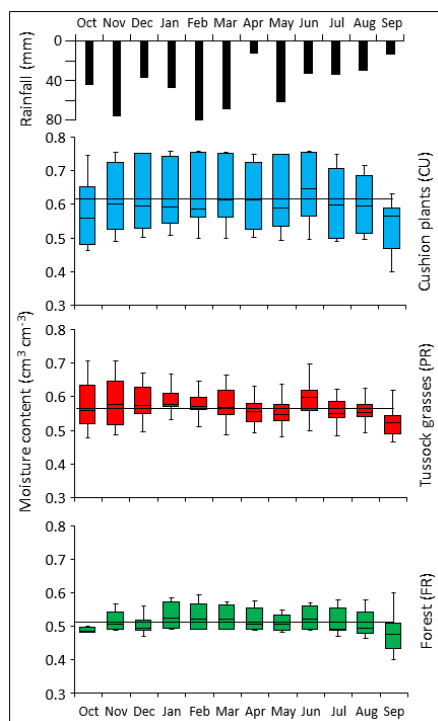
290

Figure 4: Mean monthly rainfall (mm) and mean monthly soil moisture content (cm³.cm⁻³) in soils under cushion-forming plants (mean annual VWC ± 1 SD: 0.61 ± 0.08 cm³.cm⁻³), tussock grasses (0.57 ± 0.04 cm³.cm⁻³) and forest (0.51 ± 0.03 cm³.cm⁻³).

4.3.2. Saturated hydraulic conductivity and water residence time

295   The saturated hydraulic conductivity (K_s) differed between vegetation types and between A and C horizons. The K_s was highest in the A horizons of forest soils, followed by cushion-forming plants and tussock grasses (Fig. 5, Table S2). The K_s of the C horizons was highly variable between vegetation types, with the highest values under forests and the lowest under cushion-forming plants. The saturated hydraulic conductivity was close to 0 mm.h⁻¹ in the C horizons under cushion-forming plants, indicative of the presence of an impermeable layer at the contact between soil and weathered parent material. Calculated water

300   residence time in the soils was overall high (i.e., above 200 days). Forest and tussock grasses had similar residence times of about 202 and 203 days, while soils covered by cushion-forming plants showed a longer water residence time of 231 days (Fig. 5). This points to the fact that cushion-forming plants were abundant in soils that were prone to undergo waterlogging or saturation during the rainy season, even in unusually dry years (Table S3). Given that the monitoring period was unusually dry, the differences in water residence time can be higher during normal rainfall years, and further monitoring is necessary to

305   study the potential effect of drought on water residence time.
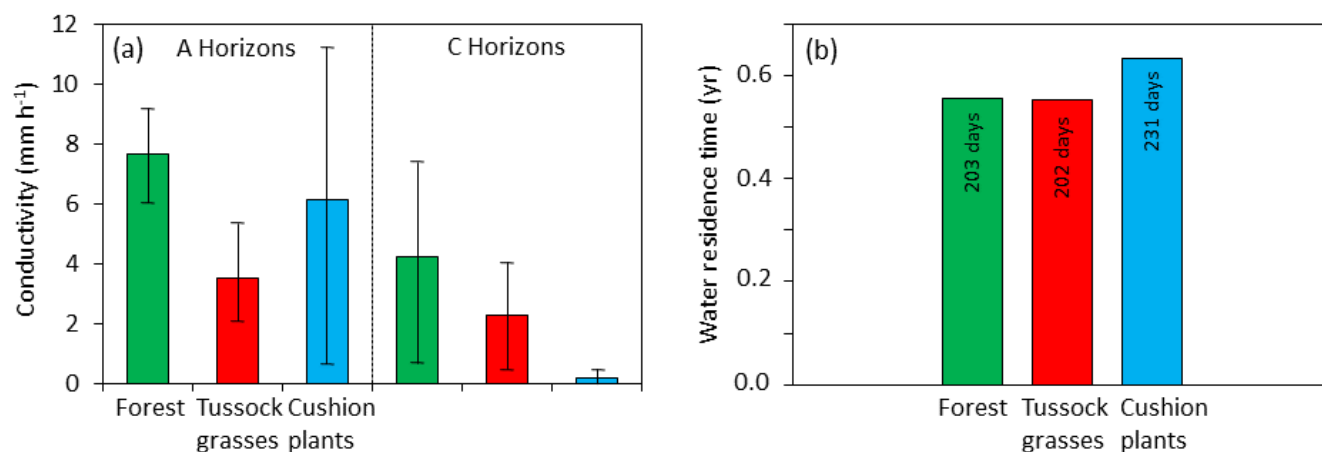
Figure 5: Mean saturated hydraulic conductivity (mm h⁻¹) and mean water residence time (yr) under forest, tussock grasses and cushion-forming plants.

310

4.4. Soil solute chemistry

The mean pH in water of the soil solutions differed between vegetation types with acidic conditions under forests (5.7 ± 0.6) and tussock grasses (6.5 ± 0.2), and near neutral conditions under cushion-forming plants (7.1 ± 0.2, Table S4). The total ionic charge of the soil solution under cushion-forming plants was about twice the concentration measured under forests and three

315 times the concentration under tussock grasses (Table 2). The major ions contributing charge in the soil solutions were rather similar between vegetation types, with Na > Ca > >Mg or K cations, and HCO_3^- >> Cl anions, although NO_3^- and K contributions were higher under forests than under cushion-forming plants and tussock grasses (Fig. S1). On annual basis, the concentrations of solute Ca, Mg, Na and Si were higher under cushion-forming plants, whereas the solute K concentration was higher under forest (Table 2). Solute Al showed the highest concentrations under forest and lowest concentrations under

320 cushion plants, whereas solute Fe showed the opposite pattern (Fig. S2). Dissolved P concentrations were close to the detection limit in the soil solution and we did not detect significant differences between vegetation types. When accounting for the difference in soil water balance between vegetation types, the Ca/Cl and Mg/Cl ratios under cushion plants were at least twice as high as under forests and tussock grasses (Fig. 6). Over one hydrological year, we noticed only minor temporal variation in Ca, Mg, Na and Si solute concentrations under forest and tussock grasses, whereas there existed large variation in these

325 concentrations under cushion plants (Fig. 7). Seasonal variation in nutrient/Cl ratios was stronger, particularly under cushion plants, where it showed clear variations throughout the year with peaks during the rainy season (Fig. S3). Solute K concentrations behaved differently than the other cations, with forests having the highest K/Cl ratio and peaks in K/Cl ratio during the rainy season. Unlike other mineral solutes, temporal variations of solute P were similar in all vegetation types.
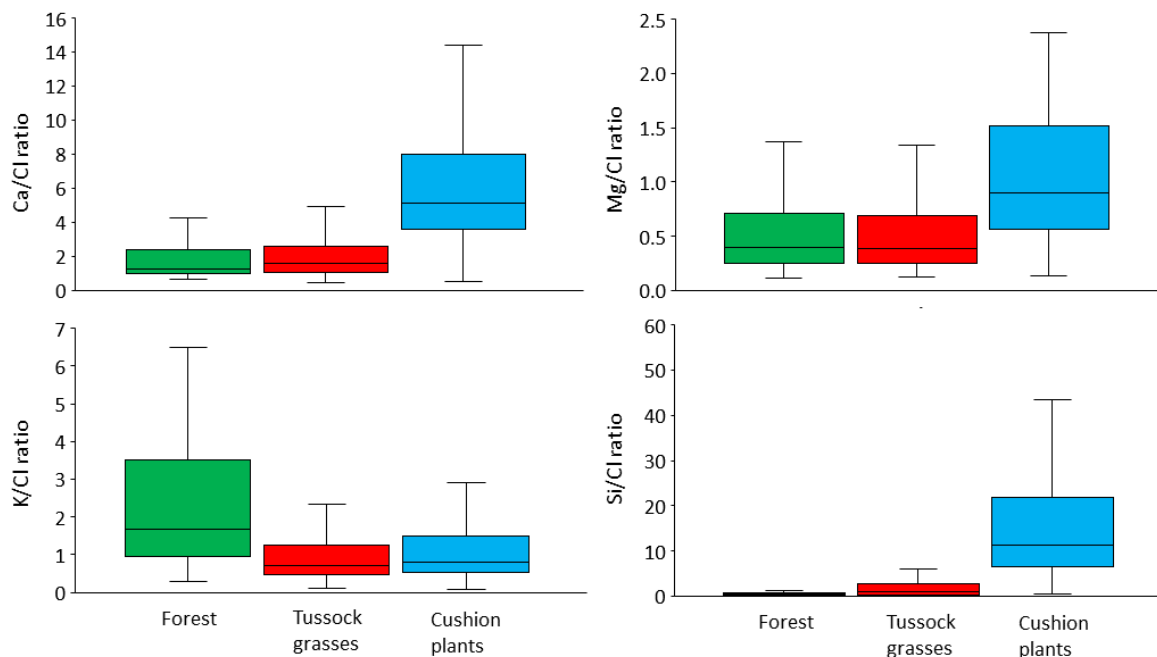
330

Figure 6: Ratio of Ca, Mg and K nutrients to Chloride in the soil solution of forests (n=7), tussock grasses (n=15) and cushion plants (n=9). An increase in the ratio indicates an enrichment of the nutrient relative to Cl, and a decrease a removal of the nutrient compared to Cl.

335

4.5. Relationship between soil moisture and solute concentrations

Soil solute concentrations varied between vegetation types and with soil moisture levels, with the exception of solute P concentrations that were consistently low at all soil moisture levels and under all vegetation types (Fig. 8). Cushion plants

340   colonized the wettest zones where the highest Ca, Mg, Na and Si solute concentrations were measured. Tussock grasses were dominant in soils with intermediate soil moisture contents and were characterized by the lowest soil solute concentrations (except Si). Forest soils had the lowest soil moisture contents over the hydrological year, and they had particularly high solute K and low Si concentrations. For all vegetation types combined, the volumetric soil water content was positively related ($r \geq$ 0.6, n = 36) to the soil solute Ca, Na, and Si concentrations, and negatively related (r = -0.6, n = 36) to the soil solute K

345   concentrations. Soil solute Mg and P concentrations were independent of the soil moisture content.
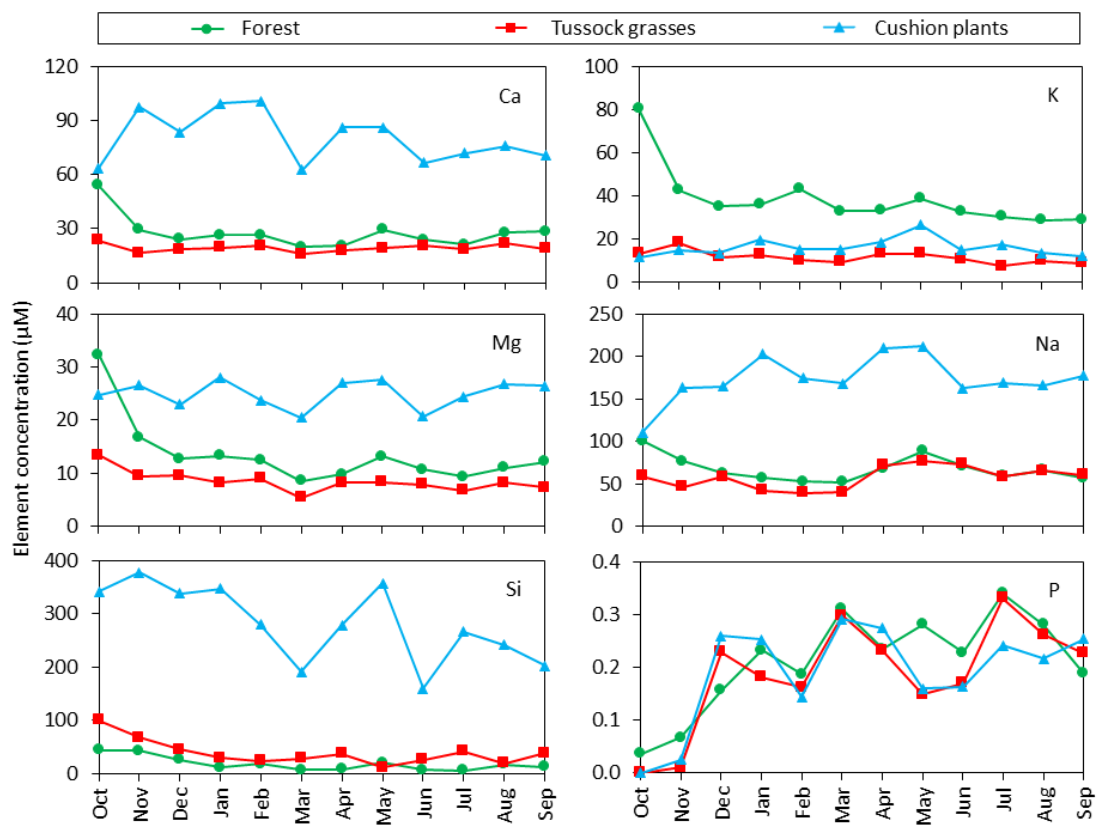
Figure 7: Temporal variation in soil solute concentrations under forest (n=7), tussock grasses (n=15) and cushion plants (n=9). The mean monthly values are plotted in the graphs. Note that the high values recorded at the beginning of the measurement period (October 2022) are likely due to the incomplete stabilization of the lysimeters before the first sampling.
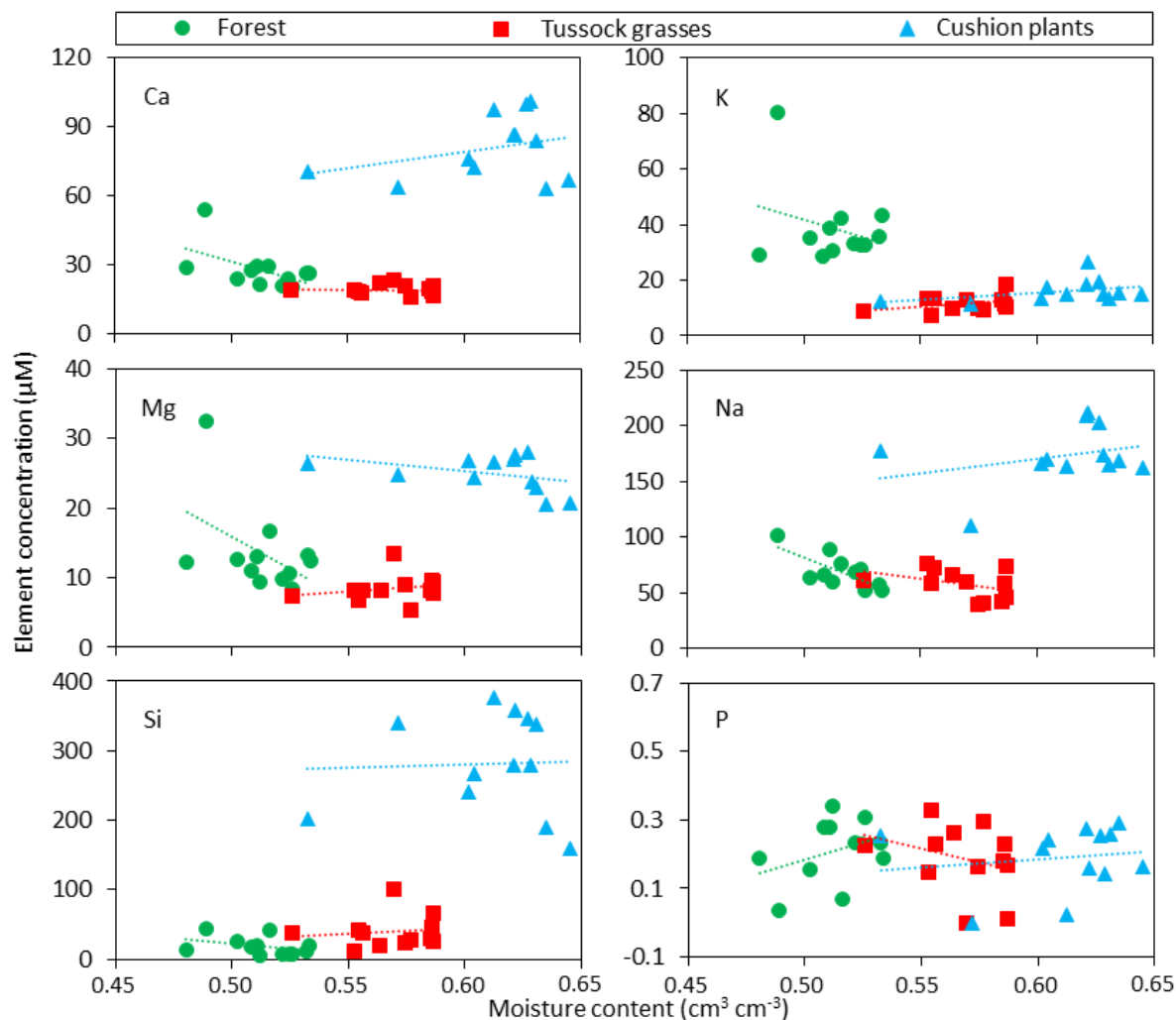
Figure 8: Relation between soil solute concentrations and soil moisture contents under forest, tussock grasses and cushion plants.

5. DISCUSSION

5.1. Soil moisture regulation by plant rooting depth

Plants employ different mechanisms to acquire water and mineral nutrients that are required for their adequate growth. Adaptation mechanisms include changes in the rooting depth so that the plants can access new sources of water and nutrients from within the weathering mantle (Schenk and Jackson, 2002). Plant rooting depth plays a key role in regulating soil-water processes (Fan et al., 2017). In the High Andes, vegetation patterns covary with slope morphology, and plant rooting depth varies with soil drainage, topographic position, and soil development.

5.1.1. Soil moisture-regulated rooting depth under cushion plants

Cushion plants are prevalent in topographic concavities and hollows where soils are seasonally waterlogged or saturated (Fig.
365   8). Although dense vegetation cover facilitates rapid soil water infiltration in the organic-rich A horizons, the water percolation
was limited by very low saturated hydraulic conductivity of the C horizon (Fig. 5). As a result, lateral soil water flow was
important under cushion plants, and it deprived the deeper subsoil of water, resulting in shallower soils due to lower weathering
rates (Molina et al., 2019). In the poorly conductive subsoil, water stagnation was evidenced by long water residence times
(Fig. 5, Table S4), and reducing conditions occurred as shown by high levels of dissolved Fe in soil solutes (Fig. S4). Cushion
370   plants are favored in these environments where the plant rooting depth is often limited by prolonged soil saturation and anoxia
during the wet season (Fig. 2). At the same time, the colonisation by cushion-forming plants leads to a positive feedback as
the relative shallow rooting of cushion plants minimizes the depth of root expansion of soil pores, enhances runoff production
and nutrient transfer operating within the upper soil horizons.

5.1.2. Soil moisture-regulated rooting depth under forests and tussock grasses

375

Forest and tussock grasses typically colonized linear and convex slopes that were characterized by soil water infiltration rates
above 2 mm.h⁻¹ in A and C horizons (Fig. 5). In t____ well-drained soils, the rooting depth followed infiltration depth and deep
roots were found at more than 1 m depth (Fig. 2). Deep soil water infiltration enabled plant root systems to develop and mine
water at depth. As shown for temperate (Rempe and Dietrich, 2018) and humid (Jobbágy and Jackson, 2007) environments,
380   deep root systems can gradually deplete soil moisture storage due to higher transpiration losses during the dry season. The
difference in soil moisture content between forests and tussock grasses was not related to the effective root depth, but likely to
be related to plant water status, i.e. the balance between water uptake by roots and water loss through transpiration from leaves.
Compared to forests, the canopy interception and evapotranspiration was lower under tussock grasses (Páez-Bimos et al.,
2023), which makes them more tolerant to water stress. In a páramo of Venezuela, Rada et al. (2019) showed that native
385   grasses were more tolerant to water stress than forest (*Polylepis sericea*) during the dry season when soil water availability
was limited due to high temperatures and evaporative demand.

5.2. Spatiotemporal variations in soil solution chemistry

As a result of strong depletion of rock-derived mineral nutrients in the nonallophanic andosols, biological processes may play
an important role in controlling soil solution chemistry. Spatial patterns of vegetation types and plant rooting depths co-occur
390   with variations in chemical weathering intensity (Molina et al., 2019) and soil solution chemistry.

5.2.1. Soil solute dynamics under cushion plants

Soil solutes under cushion-forming plants had the highest concentrations in Ca, Mg, Na and dissolved Si, as a result of low plant root uptake, and low saturated conductivity at depth (Table 2). As a result of low subsoil conductivity, soils became waterlogged during the wet season as shown by long water residence times and reduced conditions (Fig. 5). Consequently, soils under cushion plants had the lowest soil weathering intensities and neutral soil pH_{H_2O}. The plant-generated effects on soil chemistry were visible in the distribution of exchangeable Ca, Mg, and Na in the top 80 cm of the soil (Fig. 3). Exchangeable Ca and Mg were enriched in the upper soil horizon (Fig. 3), indicating that these cations were highly biocycled. Contrary to expected (Jobbagy and Jackson, 2004; White et al., 2012a), sodium was slightly enriched in the upper horizons which can be indicative of evaporation concentration of Na or biocycling of Na by cushion-forming plants. Pools of available Ca and Mg are influenced by plant biocycling, but nutrient/Cl ratios were disproportionally large in the waterlogged soils underlying the cushion plants (Fig. 6). On an annual basis, the Ca/Cl and Mg/Cl ratios in soil solutions under cushion-forming plants were 3.1 and 2.3 times higher than under forest and 3.2 and 2.5 times higher than under tussock grasses. Differences in Si/Cl ratios were even larger between vegetation types, with Si/Cl ratios under cushion-forming plants being 14.0 times higher than under forest and 6.2 times higher than under tussock grasses. Solute K and P showed different patterns, possibly due to the importance of near-surface supply of those two cations and minimal deep leaching under cushion-forming plants.

5.2.2. Soil solute dynamics under forests and tussock grasses

The water movement through deep weathering profiles, deep roots, and plant biocycling exert strong controls on solute concentrations in forest and grassland soils. The soil exchangeable Ca, Mg, and K showed the highest concentrations in the top 20 cm of soil, indicating that these cations were strongly cycled and retained by plants (Fig. 3). Biocyling of potassium can be particularly important in forest because of the relatively high nutrient demand of trees such as *Polylepis reticulata* for their physiological activities. Potassium is typically found in highest concentrations in plant tissues (Jobbagy and Jackson, 2004) and plays a major role in the osmotic balance and photosynthesis (Tripler et al., 2006).

Under forest, the soil pore waters contained remarkably high K concentrations and K/Cl ratios, given their relatively low K availability in the soil exchangeable phase and bulk soil (compared to cushion plants and tussock grasses, Fig. 3). Forest soils experienced the most severe water stress throughout the hydrological year, and tree roots effectively pump water and nutrients from deeper horizons than grasses and cushion plants (Fig. 4). Deep biological pumping of K resulted in elevated near-surface concentrations of K in forest topsoil that were 2 to 3 times higher than under tussock grasses and cushion plants.

Other soil solutes (Ca, Mg, Na and Si) had similar concentrations under forest as under tussock grasses (Table 1, Fig. 6). In these well-drained soils, the pool of plant available nutrients (e.g., Ca and Mg) are largely controlled by water percolation and leaching losses. The importance of such processes in soil nutrient depletion in volcanic soils was shown earlier by e.g.,

Chadwick et al. (2003). The remaining soil exchangeable Ca and Mg was strongly concentrated in the topsoil horizons (Fig. 3), and the result of strong biogenic control on Ca and Mg distributions. Calcium is a vital structural component of plant tissues and important for cell synthesis (McLaughlin and Wimmer, 1999), and Mg is a critical constituent of chlorophyll and many cellular enzymes and, therefore, important for photosynthesis (Shaul, 2002). In contrast to the soil exchangeable Ca and Mg distributions, Na was more concentrated at depth (Fig. 3) indicating that it was not retained in the topsoil but leached to deeper horizons. Sodium is not an essential plant nutrient and tends to be excluded by plant roots, typically resulting in greater Na concentrations in deeper soil horizons (Jobbagy and Jackson, 2001; White et al., 2012a). Under tussock grasses, there was a slight increase in exchangeable Na in the deeper horizons while there was no change in exchangeable Na concentrations under forest. Deep leaching of Na is important under forest and tussock grasses, and resulted in low Na concentrations in soil solutions. This is further confirmed by the fact that soil solute Na concentrations decreased with increasing soil moisture, i.e., during the wetter months when higher leaching losses occurred (Fig. 7).

Amongst the nutrients derived from lithogenic sources, P and K are often limiting plant development and use to be strongly biocycled (Jobbagy and Jackson, 2001). The very low soil solute P concentrations (i.e. below 1 µM) manifest a high vegetation demand of P and low solubility. The highly weathered andosols are nonallophanic and contain high levels of organometallic (Al-humus) complexes (Molina et al., 2019). Previous work in nonallophanic Andosols showed that P retention is high (i.e., > 95%) in topsoil and subsoil (Poulenard et al., 2003; Buytaert et al., 2006), which strongly limits the amount of soluble P in the soil solution, and reduces plant P uptake (Bol et al., 2016). The low soil solute P concentrations can be attributed to the strong P sorption on the Al-humus complexes, and no differences in P availability or solute concentrations were observed between vegetation types (Fig. S2).

6. CONCLUSION

The páramo landscape in the High Andes forms a vegetation mosaic of bunch-grasses, cushion-forming plants and forests. This study on soil-water-vegetation interactions evaluated the association between vegetation, soil hydrology and mineral nutrient availability at the landscape scale. In the highly nutrient-depleted nonallophanic Andosols, the plant rooting depth varies with drainage and soil moisture conditions. Topographic depressions that are seasonally waterlogged mainly comprise shallow soils, and shallow-rooted plants such as cushion-forming vegetation. In comparison, hillslopes contain deeper and better drained weathering profiles, and are colonised by bunch grasses and trees whose rooting systems extend to more than 100 cm depth. The type of vegetation is a relevant indicator of the availability of rock-derived nutrients in the soil solutions. Soils under cushion-forming plants had more than 2.5 times higher solute concentrations of Ca, Mg, Na and Si than forest and tussock grasses, where intense cation leaching and plant nutrient retention depressed the lithogenic solute concentrations. Potassium clearly showed different behaviour than the before-mentioned cations: while the total K stock and exchangeable K in the soil were lowest under forests, their soil solute K concentrations and K/Cl ratios were 2 to 3 times higher than under cushion-forming plants or tussock grasses. The soil solute chemistry revealed patterns in plant available nutrients that are not

solely mimicking the distribution of total rock-derived nutrients or the exchangeable nutrient pool, but that clearly resulted
from strong biocycling of cations and removal of nutrients from the soil by plant uptake and deep leaching.

Our findings have important implications for future management of Andean paramo ecosystems where vegetation type distributions are dynamically changing as a result of warming temperatures and anthropogenic disturbances. results put forward that vegetation communities are related to soil chemical weathering extent, hydro-physical properties and hydrochemistry of soil pore waters. As such, changes in vegetation distributions will not only lead to changes in soil hydrology and solute geochemistry but may also lead on to complex changes in weathering rates and solute export downstream with effects on nutrient availability and, hence, aquatic ecology of Andean rivers and high-mountain lakes. Our results ask for further evaluations of vegetation-related soil water and solute fluxes, including coupling of soil moisture and solute chemistry with water fluxes and upscaling of hydrochemistry from soil profile to ecosystem scale.

Data availability

All data used in this paper are archived and will be publicly available in the UCLouvain DataVerse upon final publication of the paper.

Supplement

The supplement related to this article contains four supplementary figures and four supplementary tables. The pdf containing the supplements is provided with the submission, and will be available online upon final publication of the paper.

Author contributions

Conceptualization: AM, EV, VV: experimental design: AM, VV; data collection: AM, SZ; data validation: AM, OC, MC, VV; interpretation and analyses: AM, VV, OC, EV; funding acquisition: AM, VV; project administration: AM, EV; writing – original draft: AM, VV; writing – review and editing: all authors.

Competing interests

At least one of the (co-)authors is a member of the editorial board of Biogeosciences.

Acknowledgements

We thank Marco Ramirez and Oscar Morales for assistance and support during the field campaigns, and are grateful for the
480 help of several undergraduate students (Juan Barahona, Tanya Contreras and René Fernández) of the Universidad de Cuenca.
Eduardo Tacuri and Mateo López realised the UAV flights over the study area, and provided the very high resolution
topography and imagery. We acknowledge Sandra Barros and Javier Fernández de Cordoba of ETAPA EP (Empresa Pública
Municipal de Telecomunicaciones, Agua Potable, Alcantarillado y Saneamiento de Cuenca) for continued support of our
research activities in the High Andean headwater basins, and want to express our appreciation to Felipe Cisneros of PROMAS
485 (Programa para el Manejo del Agua y del Suelo, Universidad de Cuenca) for continued support.

Financial support

Armando Molina received a Georg Forster Fellowship for Postdoctoral Researchers (3.2-ECU/1138588 STP) from the
Alexander von Humboldt Foundation, and a Prometeo grant from the Secretaría de Educación Superior, Ciencia, Tecnología
e Innovación from the Ecuadorian government. Additional support was provided by the research cooperation projects
490 "Strengthening the scientific and technological capacities to implement spatially integrated land and water management
schemes adapted to local socio-economic, cultural and physical settings" (CUD PIC-09 Ecuador) and "Linking Global Change
with Soil and Water Conservation in the High Andes" (ARES PRD-17 ParamoSus) funded by the Académie de Recherche et
d'Enseignement Supérieur de la Fédération Wallonie-Bruxelles (ARES) of Belgium.

References

495 Amundson, R., Richter, D. D., Humphreys, G. S., Jobbágy, E. G., and Gaillardet, J.: Coupling between Biota and Earth
Materials in the Critical Zone, Elements, 3, 327-332, https://doi.org/10.2113/gselements.3.5.327, 2007.

Amundson, R.: An Introduction to the Biogeochemistry of Soils., Cambridge, UK, Cambridge University Press, ISBN: 978-
1-108-83126-0, 2021.

Beate, B., Monzier, M., Spikings, R., Cotton, J., Silva, J., Bourdon, E., and Eissen, J . P.: Mio-Pliocene adakite generation
500 related to flat subduction in southern Ecuador: The Quimsacocha volcanic center, Earth. Planet. Sc. Lett., 192, 561-570,
https://doi.org/10.1016/S0012-821X(01)00466-6, 2001.

Bol, R., Julich, D., Brödlin, D., Siemens, J., Kaiser, K., Dip- pold, M. A., Spielvogel, S., Zilla, T., Mewes, D., von Blanck-
enburg, F., Puhlmann, H., Holzmann, S., Weiler, M., Amelung, W., Lang, F., Kuzyakov, Y., Feger, K. H., Gottselig, N.,
Klumpp, E., Missong, A., Winkelmann, C., Uhlig, D., Sohrt, J., von Wilpert, K., Wu, B., and Hagedorn, F.: Dissolved and
505 colloidal phosphorus fluxes in forest ecosystems – an almost blind spot in ecosystem research, J. Plant Nutr. Soil Sc., 179,
425–438, https://doi.org/10.1002/jpln.201600079, 2016.

Boxman, A. W., Peters, R. C., and Roelofs, J. G.: Long term changes in atmospheric N and S throughfall deposition and effects on soil solution chemistry in a Scots pine forest in the Netherlands, Environ. Pollut., 156, 1252-1259, https://doi:10.1016/j.envpol.2008.03.017, 2008.

510 Brantley, S. L. and White, A. F.: Approaches to modeling weathered regolith, Reviews in Mineralogy and Geochemistry., 70, 435-484, https://doi.org/10.2138/rmg.2009.70.10, 2009.

Brantley, S. L., Eissenstat, D. M., Marshall, J. A., Godsey, S. E., Balogh-Brunstad, Z., Karwan, D. L., Papuga, S. A., Roering, J., Dawson, T. E., Evaristo, J., Chadwick, O., McDonnell, J. J., and Weathers, K. C.: Reviews and syntheses: On the roles trees play in building and plumbing the critical zone, Biogeosciences, 14, 5115–5142, https://doi.org/10.5194/bg-14-515 5115-2017, 2017.

Buss, H. L., Chapela Lara, M., Moore, O. W., Kurtz, A. C., Schulz, M. S., and White, A. F.: Lithological influences on contemporary and long-term regolith weathering at the Luquillo Critical Zone Observatory, Geochim. Cosmochim. Ac., 196, 224–251, https://doi.org/10.1016/j.gca.2016.09.038, 2017.

Buytaert, W., De Bièvre, B., Wyseure, G., and Deckers, J.: The effect of land use changes on the hydrological behaviour of 520 Histic Andosols in south Ecuador, Hydrol. Process., 19: 3985–3997, https://doi.org/10.1002/hyp.5867, 2005.

Buytaert, W., Deckers, J., and Wyseure, G.: Description and classification of nonallophanic Andosols in south Ecuadorian alpine grasslands (páramo), Geomorphology, 73, 207–221, https://doi.org/10.1016/j.geomorph.2005.06.012, 2006.

Canadell, J., Jackson, R. B., Ehleringer, J. B., Mooney, H. A., Sala, O. E., and Schulze, E. D.: Maximum rooting depth of vegetation types at the global scale, Oecologia, 108, 583-595, https://doi.org/10.1007/BF00329030, 1996.

525 Carrillo-Rojas, G., Silva, B., Rollenbeck, R. Célleri, R., and Bendix, J.: The breathing of the Andean highlands: Net ecosystem exchange and evapotranspiration over the páramo of southern Ecuador, Agr. Forest Meteorol, 265, 30-47, https://doi.org/10.1016/j.agrformet.2018.11.006, 2019.

Chadwick, O. A., Derry, L. A., Vitousek, P. M., Huebert, B. J., and Hedin, L. O.: Changing sources of nutrients during four million years of ecosystem development, Nature, 397, 491-497, https://doi.org/10.1038/17276, 1999.

530 Chadwick, O. A., Gavenda, R. T., Kelly, E. F., Ziegler, K., Olson, C. G., Elliott, W. C., and Hendricks, D. M.: The impact of climate on the biogeochemical functioning of volcanic soils, Chem. Geol., 202, 195-223, https://doi.org/10.1016/j.chemgeo.2002.09.001, 2003.

Clapuyt, F., Vanacker, V., Van Oost, K., 2016. Reproducibility of UAV-based earth topography reconstructions based on Structure-from-Motion algorithms. Geomorphology 260, 4–15. https://doi.org/10.1016/j.geomorph.2015.05.011.

535 Coblentz, D. and Keating, P. L.: Topographic controls on the distribution of tree islands in the high Andes of south-western Ecuador, Journal of Biogeography, 35, 2026-2038, https://doi.org/10.1111/j.1365-2699.2008.01956.x, 2008.

Comas, X., Terry, N., Hribljan, J. A., Erik Lilleskov, E., Suarez, E., Chimner, R. A., and Kolka, R.: Estimating belowground carbon stocks in peatlands of the Ecuadorian páramo using ground penetrating radar (GPR), J. Geophys. Res.-Biogeo., 122, 370-386, https://doi.org/10.1002/2016JG003550, 2017.

540   Cramer, M. D., Hoffmann, V., and Verboom, G. A.: Nutrient availability moderates transpiration in Ehrharta calycina, New Phytol., 179, 1048-1057, https://doi.org/10.1111/j.1469-8137.2008.02510.x, 2008.

Crawley, M. J.: The R book, John Wiley and Sons Limited, Chichester, UK, 2009.

Dawson, T. E., Hahm, W. J., and Crutchfield-Peters, K.: Digging deeper: what the critical zone perspective adds to the study of plant ecophysiology, New Phytol., 226, 666-671, https://doi.org/10.1111/nph.16410, 2020.

545   Dixon, J. L., Chadwick, O. A., and Vitousek, P. M.: Climate-driven thresholds for chemical weathering in postglacial soils of New Zealand, J. Geophys. Res.-Earth Surf., 121, 1619-1634, https://doi.org/10.1002/2016JF003864, 2016.

Fan, Y., Miguez-Macho, G., Jobbágy, E. G., Jackson, R. B., and Otero-Casal, C.: Hydrologic regulation of plant rooting depth, P. Natl. Acad. Sci. USA, 114, 10572-10577, https://doi.org/10.1073/pnas.1712381114, 2017.

Hansen, B. C., Rodbell, D., Seltzer, G., León, B., Young, K., and Abbott, M.: Late-glacial and Holocene vegetational history from two sites in the western Cordillera of southwestern Ecuador, Palaeogeogr. Palaeoecol., 194, 79–108, doi:10.1016/S0031-0182(03)00272-4, 2003.

550

Hasenmueller, E. A., Gu, X., Weitzman, J. N., Adams, T. S., Stinchcomb, G. E., Eissenstat, D. M., Drohan, P. J., Brantley, S. L., and Kaye, J. P.: Weathering of rock to regolith: The activity of deep roots in bedrock fractures, Geoderma, 300, 11-31, https://doi.org/10.1016/j.geoderma.2017.03.020, 2017.

555   Hedin, L. O., Vitousek, P. M., and Matson, P. A.: Nutrient losses over four million years of tropical forest development, Ecology, 84, 2231-2255, https://doi.org/10.1890/02-4066, 2003.

Hobbie, S. E.: Effects of plant-species on nutrient cycling, Trends Ecol. Evol., 7, 336-339, https://doi.org/10.1016/0169-5347(92)90126-V, 1992.

Hribljan, J. A., Suárez, E., Heckman, K. A., Lilleskov, E. A., and Chimner, R. A.: Peatland carbon stocks and accumulation
560   rates in the Ecuadorian paramo, Wetlands Ecol. Manage., 24, 113-127, https://doi.org/10.1007/s11273-016-9482-2, 2016.

Jackson, R. B., Schenk, H. J., Jobbágy, E. G., Canadell, J., Colello, G. D., Dickinson, R. E., Field, C. B., Friedlingstein, P., Heimann, M., Hibbard, K., Kicklighter, D. W., Kleidon, A., Neilson, R. P., Parton, W. J., Sala, O. E., and Sykes, M. T.: Belowground consequences of vegetation change and their treatment in models, Ecological Applications, 10, 470-483, https://doi.org/10.1890/1051-0761(2000)010[0470:BCOVCA]2.0.CO;2, 2000.

565   Jackson, R. B., Banner, J. L., Jobbágy, E. G., Pockman, W. T., and Wall, D. H.: Ecosystem carbon loss with woody plant invasion of grasslands, Nature, 418, 623-626, https://doi.org/10.1038/nature00910, 2002.

Jantz, N. and Behling, H.: A Holocene environmental record reflecting vegetation, climate, and fire variability at the Páramo of Quimsacocha, southwestern Ecuadorian Andes, Vegetation History and Archaeobotany., 21, 169-185, https://doi.org/10.1007/s00334-011-0327-x, 2012.

570   Jobbágy, E. G. and Jackson, R. B.: The distribution of soil nutrients with depth: Global patterns and the imprint of plants, Biogeochemistry, 53, 51-77, https://doi.org/10.1023/A:1010760720215, 2001.

Jobbágy, E. G. and Jackson, R. B.: The uplift of soil nutrients by plants: Biogeochemical consequences across scales, Ecology, 85, 2380-2389, https://doi.org/10.1890/03-0245, 2004.

Jobbágy, E. G. and Jackson, R. B.: Groundwater and soil chemical changes under phreatophytic tree plantations, J. Geophys. Res.-Biogeo., 112, G02013, https://doi.org/10.1029/2006JG000246, 2007.

Kelly, E. F., Chadwick, O. A., and Hilinski, T. E.: The effects of plants on mineral weathering, Biogeochemistry, 42, 21-53, https://doi.org/10.1023/A:1005919306687, 1998.

Klute, A.: Water Retention: Laboratory Methods, in: Methods of Soil Analysis: Part 1 Physical and Mineralogical Methods, edited by: Klute, A., Soil Science Society of America, American Society of Agronomy, Madison, WI, USA, 635–662, https://doi.org/10.2136/sssabookser5.1.2ed.c26, 1986.

Kurniawan, S., Corre, M. D., Matson, A. L., Schulte- Bisping, H., Utami, S. R., van Straaten, O., and Veldkamp, E.: Conversion of tropical forests to smallholder rubber and oil palm plantations impacts nutrient leaching losses and nutrient retention efficiency in highly weathered soils, Biogeosciences, 15, 5131-5154, https://doi.org/10.5194/bg-15-5131-2018, 2018.

Landeweert, R., Hoffland, E., Finlay, R. D., Kuyper, T. W., and van Breemen, N.: Linking plants to rocks: ectomycorrhizal fungi mobilize nutrients from minerals, Trends Ecol. Evol., 16, 248-254, https://doi.org/10.1016/S0169-5347(01)02122-X, 2001.

Lazo, P.X., Mosquera, G.M., McDonnell, J.J., and Crespo, P.: The role of vegetation, soils, and precipitation on water storage and hydrological services in Andean páramo catchments, J. Hydrol., 572, 805-819, https://doi.org/10.1016/J, 2019.

Marín, F., Dahik, C., Mosquera, G., Feyen, J., Cisneros, P., and Crespo, P.: Changes in soil hydro-physical properties and SOM due to pine afforestation and grazing in Andean environments cannot be generalized, Forests, 10, 1-23, https://doi.org/10.3390/f10010017, 2018.

McLaughlin, S. B. and Wimmer, R.: Calcium physiology and terrestrial ecosystem processes, New Phytol., 142, 373-417, 1999.

Minaya, V., Corzo, G., Romero-Saltos, H., van der Kwast, J., Lantinga, E., Galárraga-Sánchez, R., and Mynett, A.: Altitudinal analysis of carbon stocks in the Antisana páramo, Ecuadorian Andes, Journal of Plant Ecology, 9, 553-563, https://doi.org/10.1093/jpe/rtv073, 2016.

Molina, A., Vanacker, V., Corre, M. D., and Veldkamp, E.: Patterns in soil chemical weathering related to topographic gradients and vegetation structure in a high Andean tropical ecosystem, J. Geophys. Res.-Earth Surf., 124, 666-685, https://doi.org/10.1029/2018JF004856, 2019.

Mora, D. E. and Willems, P.: Decadal oscillations in rainfall and air temperature in the Paute River basin-southern Andes of Ecuador, Theoretical and Applied Climatology., 108, 267-282, https://doi.org/10.1007/s00704-011-0527-4, 2012.

Mosquera, P. V., Hampel, H., Vázquez, R. F., and Catalan, J.: Water chemistry variation in tropical high-mountain lakes on old volcanic bedrocks, Limnol. Oceanogr., 67, 1522–1536, https://doi.org/10.1002/lno.12099, 2022.

Nieminen, T. M., Derome, K., Meesenburg, H., and De Vos, B.: Chapter 16-Soil Solution: Sampling and Chemical Analyses, Developments in Environmental Science., 12, 301-315, https://doi.org/10.1016/B978-0-08-098222-9.00016-9, 2013.

Olshansky, Y., Knowles, J. F., Barron-Gafford, G. A., Rasmussen, C., Abramson, N., and Chorover, J.: Soil fluid biogeochemical response to climatic events, J. Geophys. Res.-Biogeo., 124, 2866-2882, https://doi.org/10.1029/2019JG005216, 2019.

Páez-Bimos, S., Villacís, M., Morales, O., Calispa, M., Molina, A., Salgado, S., De Bièvre, B., Muñoz, T., and Vanacker, V.:
610 Vegetation effects on soil pore structure and hydraulic properties in volcanic ash soils of the high Andes, Hydrol., Process, 36, e14678, https://doi.org/10.1002/hyp.14678, 2022.

Páez-Bimos, S., Molina, A., Calispa, M., Dellmelle, P., Lahuatte, B., Villacís, M., Muñoz, T., and Vanacker, V.: Soil–vegetation–water interactions controlling solute flow and chemical weathering in volcanic ash soils of the high Andes, Hydrol. Earth Syst. Sci, 27, 1507–1529, https://doi.org/10.5194/hess-27-1507-2023.

615 Podwojewski, P. and Poulenard, J.: En los suelos del páramo del Ecuador, Serie Páramo 5, GTP/Abya Yala, Quito, Ecuador, ISBN: 9978-04-591-0, 2000.

Porder, S. and Chadwick, O. A.: Climate and soil-age constraints on nutrient uplift and retention by plants, Ecology, 90, 623-636, https://doi.org/10.1890/07-1739.1, 2009.

Poulenard, J., Podwojewski, P., and Herbillon, A. J.: Characteristics of non-allophanic andisols with hydric properties from
620 the Ecuadorian paramos, Geoderma, 117, 267–281, https://doi.org/10.1016/s0016-7061(03)00128-9, 2003.

Rada, F., Azocar, A., and García-Nuñez, C.: Plant functional diversity in tropical Andean paramos, Plant Ecology and Diversity., 12, 539-553, https://doi.org/10.1080/17550874.2019.1674396, 2019.

Ramsay, P. M.: The Páramo Vegetation of Ecuador: the community ecology, dynamics and productivity of tropical grasslands in the Andes, PhD thesis 1-274, University of Wales, UK, 1992.

625 Rempe, D. M. and Dietrich, W. E.: Direct observations of rock moisture, a hidden component of the hydrologic cycle, P. Natl. Acad. Sci. USA, 115, 2664-2669, https://doi.org/10.1073/pnas.1800141115, 2018.

Rodbell, D. T., Bagnato, S., Nebolini, J. C., Seltzer, G. O., and Abbott, M. B.: A Late-Glacial-Holocene tephrochronology for glacial lakes in southern Ecuador, Quaternary Research, 57, 343-354, https://doi.org/10.1006/qres.2002.2324, 2002.

Schenk, H. J. and Jackson, R. B.: Rooting depths, lateral root spreads and below-ground/above-ground allometries of plants
630 in water-limited ecosystems, Journal of Ecology, 90, 480-494, https://www.jstor.org/stable/3072232, 2002.

Schwendenmann, L. and Veldkamp, E.: The role of dissolved organic carbon, dissolved organic nitrogen and dissolved inorganic nitrogen in a tropical wet forest ecosystem, Ecosystems, 8, 339-351, https://doi.org/10.1007/s10021-003-0088-1, 2005.

Shaul, O.: Magnesium transport and function in plants: the tip of the iceberg, Biometals, 15, 307-321,
635 https://doi.org/10.1023/A:1016091118585, 2002.

Tenorio, G. E., Vanacker, V., Campforts, B., Álvarez, L., Zhiminaicela, S., Vercruysse, K., Molina, A., and Govers, G.: Tracking spatial variation in river load from Andean highlands to inter-Andean valleys, Geomorphology, 308, 175–189, https://doi.org/10.1016/j.geomorph.2018.02.009, 2018.

Tonneijck, F. H., Jansen, B., Nierop, K. G. J., Verstraten, J. M., Sevink, J., and de Lange, L.: Towards understanding of carbon
640   stocks and stabilization in volcanic ash soils in natural Andean ecosystems of northern Ecuador, Eur. J. Soil Sci., 61, 392–405,
https://doi.org/10.1111/j.1365-2389.2010.01241.x, 2010.

Tripler, C. E., Kaushal, S. S., Likens, G. E., and Walter, M. T.: Patterns in potassium dynamics in forest ecosystems, Ecology
Letters, 9, 451-466, https://doi.org/10.1111/j.1461-0248.2006.00891.x, 2006.

Uhlig, D., Schuessler, J. A., Bouchez, J., Dixon, J. L., and von Blanckenburg, F.: Quantifying nutrient uptake as driver of rock
645   weathering in forest ecosystems by magnesium stable isotopes, Biogeosciences, 14, 3111-3128, https://doi.org/10.5194/bg-
14-3111-2017, 2017.

Uhlig, D., Amelung, W., and von Blanckenburg, F.: Mineral nutrients sourced in deep regolith sustain long-term nutrition of
mountainous   temperate   forest   ecosystems,   Global   Biogeochem.   Cy.,   34,   e2019GB006513,
https://doi.org/10.1029/2019GB006513, 2020.

650   van Dam, J. C., Stricker, J. N. M., and Droogers, P.: Inverse method to determine soil hydraulic functions from multistep
outflow experiments, Soil Sci. Soc. Am. J., 58(3), 647–652. https://doi.org/10.2136/sssaj1994.03615995005800030002x,
1994.

van Genuchten, M. T.: A closed-form equation for predicting the hydraulic properties of unsaturated soils, Soil Sci. Soc. Am.
J., 44, 892-898, 1980.

655   van Hoorn, J. W.: Determining hydraulic conductivity with the inversed auger hole and infiltrometer methods, Proceedings of
the International Drainage Workshop, 150-249, International Institute for Land Reclamation and Improvement, Wageningen,
the Netherlands, 1979.

Vitousek, P., Chadwick, O., Matson, P., Allison, S., Derry, L., Kettley, L., Luers, A., Mecking, E., Monastra, V., and Porder,
S.: Erosion and the Rejuvenation of Weathering-derived Nutrient Supply in an Old Tropical Landscape, Ecosystems, 6, 762-
660   772, https://doi.org/10.1007/s10021-003-0199-8, 2003.

Vitousek, P. M. Nutrient Cycling and Limitation: Hawaii as a Model System. USA: Princeton University Press, ISBN: 0-691-
11579-6, 2004.

White, A. F., Schulz, M. S., Stonestrom, D. A., Vivit, D. V., Fitzpatrick, J., Bullen, T. D., Maher, K., and Blum, A. E.: Chemical
weathering of a marine terrace chronosequence, Santa Cruz, California. Part II: Solute profiles, gradients and the comparisons
665   of   contemporary   and   long-term   weathering   rates,   Geochim.   Cosmochim.   Acta,   73,   2769–2803,
https://doi.org/10.1016/j.gca.2009.01.029, 2009.

White, A. F., Schulz, M. S., Vivit, D. V., Bullen, T. D., and Fitzpatrick, J.: The impact of biotic/abiotic interfaces in mineral
nutrient cycling: a study of soils of the Santa Cruz chronosequence, California, Geochim. Cosmochim. Ac., 77, 62-85,
https://doi.org/10.1016/j.gca.2011.10.029, 2012a.

670   White, A. F., Vivit, D. V., Schulz, M. S., Bullen, T. D., Evett, R. R., and Aagar- wal, J.: Biogenic and pedogenic controls on
Si distributions and cycling in grasslands of the Santa Cruz soil chronosequence, California, Geochim. Cosmochim. Ac., 94,
72-94, https://doi.org/10.1016/j.gca.2012.06.009, 2012b.

White, S.: Grass páramo as hunter-gatherer landscape, The Holocene, 23, 898-915, https://doi.org/10.1177/0959683612471987, 2013.

675 Zhang, H., Aldana-Jague, E., Clapuyt, F., Wilken, F., Vanacker, V., Van Oost, K., 2019. Evaluating the potential of post-processing kinematic (PPK) georeferencing for UAV- based structure-from-motion (SfM) photogrammetry and surface change detection. Earth Surf. Dynam. 7, 807–827. https://doi.org/10.5194/esurf-7-807-2019.